AFRL-SR-AR-TR-08-0216

REPORT DOCUMENTATION PAGE

1. AGENCY USE ONLY (*Leave Blank*)	2. REPORT DATE	3. REPORT TYPE AND DATES COVERED
	April 4, 2008	Final Technical, 01/01/05 – 12/31/07

4. TITLE AND SUBTITLE
Measurements of Secondary Electron Yield from Materials with Application to Depressed Collectors

5. FUNDING NUMBERS
FA90550-05-1-0051

6. AUTHORS
Edl Schamiloglu and Mark Gilmore

7. PERFORMING ORGANIZATION NAME(S) AND ADDRESS(ES)
University of New Mexico
MSC01 1100
Department of Electrical and Computer Engineering
Albuquerque, NM 87131-1356

8. PERFORMING ORGANIZATION REPORT NUMBER

9. SPONSORING / MONITORING AGENCY NAME(S) AND ADDRESS(ES)
AFOSR/NE
875 North Randolph Street, Suite 325
Arlington, VA 22203
Dr Robert Barker

10. SPONSORING / MONITORING AGENCY REPORT NUMBER

11. SUPPLEMENTARY NOTES

12a. DISTRIBUTION / AVAILABILITY STATEMENT
Unlimited
Distribution A: Approved for Public Release

12b. DISTRIBUTION CODE
AFOSR/NE

13. ABSTRACT *(Maximum 200 words)*

This final technical report reviews the research activities during the period of this grant, emphasizing the final year. The key finding of our study is that the total incident electron dose is a critical parameter affecting secondary electron emission (SEE). A completely automated experimental set-up was implemented that allowed for measurement of secondary electron yield (SEY) as a function of beam energy, angle of incidence of primary electrons, electron dose, and time. We present SEY data for copper, plasma-sprayed boron carbide, and titanium nitride samples with principal attention given to the dose dependence. Experiments were conducted in the energy range 5 – 1000 eV using DC voltages. Modified empirical formulas are proposed that incorporate the dose effect and match the experimental measurements.

14. SUBJECT TERMS	15. NUMBER OF PAGES
Secondary electron emission, depressed collectors, high power microwaves, gyrotrons, dose effect	41
	16. PRICE CODE

17. SECURITY CLASSIFICATION OF REPORT	18. SECURITY CLASSIFICATION OF THIS PAGE	19. SECURITY CLASSIFICATION OF ABSTRACT	20. LIMITATION OF ABSTRACT
Unclassified	Unclassified	Unclassified	None

THE UNIVERSITY of NEW MEXICO SCHOOL of ENGINEERING

Department of Electrical & Computer Engineering

"Measurements of Secondary Electron Yield from Materials with Application to Depressed Collectors"

Final Technical Report
1 January 2005 – 31 December 2007

4 April 2008

Submitted by:

Edl Schamiloglu — Principal Investigator and Professor
Department of Electrical and Computer Engineering
University of New Mexico
Albuquerque, NM 87131
Tel. (505) 277-4423
Fax: (505) 277-1439
e-mail: edl@ece.unm.edu

and:

Mark Gilmore – Co-Principal Investigator and Assistant Professor
Department of Electrical and Computer Engineering
University of New Mexico
Albuquerque, NM 87131
Tel. (505) 277-2579
Fax: (505) 277-1439
e-mail: gilmore@ece.unm.edu

TABLE OF CONTENTS

LIST OF FIGURES

I. INTRODUCTION

Secondary electron emission (SEE) is the liberation of electrons from a material due to bombardment by a beam of charged particles. An important parameter used to measure the secondary emission ability of a substance is the secondary electron yield (SEY), defined as the ratio of liberated or secondary electrons to incident or primary electrons [1], and commonly denoted by δ.

There are many practical applications where a large SEY is desirable (as in photomultiplier tubes and image intensifiers). However, there are also situations where a large SEY is problematic. One such undesirable manifestation of SEE is in collectors of high power microwave (HPM) sources. HPM sources (such as gyrotrons and gyroklystrons) may suffer deleterious effects due to secondary electrons produced from surfaces exposed to the spent electron beam. The device's efficiency in such cases can be significantly increased by reducing the SEY from collectors. Our primary motivation is to investigate low SEY materials which could potentially be used in collectors of HPM sources.

A generalized theory of SEE from all materials (metals, semiconductors, dielectrics, *etc.*) presents an overwhelmingly complicated problem. Even when limiting the discussion to only metals, poor agreement is observed between proposed classical and quantum mechanical theories and many published experimental results (see, for example, [1] and references therein). Such disagreement may be attributed to missing experimental details. It is in this regard that we believe an important aspect to the measurement of secondary electron emission needs more attention, specifically, the "dose effect." In essence, the dose effect refers to the dependence of SEY on dose (charge per unit area) incident on the sample. The dose effect has, at best, been sparingly acknowledged and documented in very few recent works such as Baglin *et al.* [2] and Kirby *et al.* [3]. The results presented in this final report indicate electron dose as a necessary parameter to more completely and accurately describe the SEY of a given material. Previously unexplained temporal variations in SEY [4,5] will be shown to be a consequence of the dose effect. Apart from our principal focus on the dose effect, experimental results presented here also include variation of SEY as a function of time (t) and angle of incidence of primary electrons θ. Emperical relationships obtained from our experiments are used to modify formulas presented in Vaughan [6] and Lye and Dekker [7].

II. SUMMARY OF SEE THEORIES

A generic SEY curve is shown in Fig. 1. δ_m is the maximum yield and E_m is the energy at maximum yield. E_I and E_{II} represent cross-over energies, *i.e.* points at which the SEY is unity.

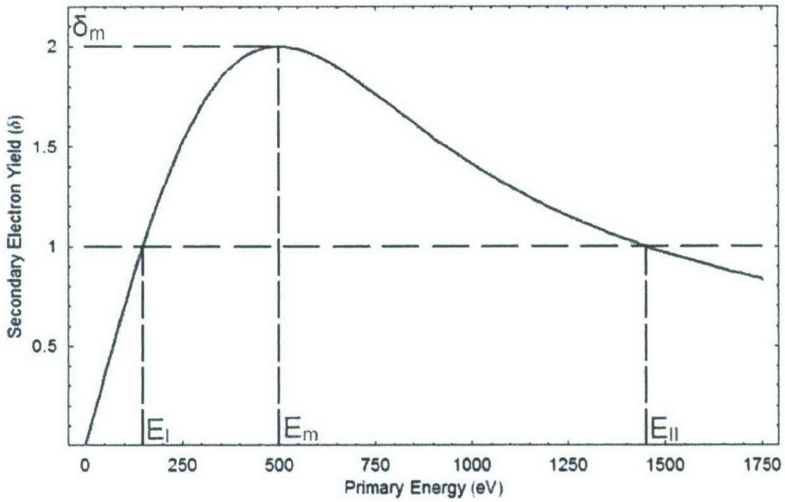

Figure 1. Typical SEY curve showing variation with primary energy.

The existence of a universal reduced yield curve $\left(\delta/\delta_m \; vs. \; E/E_m\right)$ in the case of metals (this report limits discussion to SEE from metals, since the application requires this) was first proposed by Baroody [8]. This section focuses on three classical theories relevant to the work presented in this report. Equations relating $\left(\delta/\delta_m\right)$ to $\left(E/E_m\right)$ as given by Lye and Dekker [7], Dionne [9,10], and Vaughan [6,11] are highlighted next.

Lye and Dekker's formulation is an extension of the theory originally proposed by Bruining [1]. It is assumed the SEY may be derived from the generic expression

$$\delta = \int_0^\infty n(x, E_p) f(x) dx \tag{1}$$

where, $n(x, E_p)$ represents the number of secondaries produced per incident primary of initial energy E_p in a layer of thickness dx at a depth x below the surface. $f(x)$ is the probability that a secondary produced at x arrives at and escapes from the surface. In developing a theory from Eq. (1), Bruining assumes:

1. $n(x,E_p)$ is proportional to energy loss of the primary beam per unit path length, *i.e.* $n(x,E_p) = -K\,dE_p/dx$, evaluated per incident particle (perpendicular incidence assumed).

2. $f(x)$ is given by $\exp(-\alpha x)$, where $1/\alpha$ corresponds to a common effective range of secondaries in the solid under consideration.

Lye and Dekker additionally assume:

3. Primary energy losses are governed by a power law of the form

$$dE_p/dx = -A/E_p^n(x), \tag{2}$$

where n is an arbitrary constant and A characterizes the material.

4. The probability for an electron of a given initial energy E_p to be transmitted through a solid layer of thickness x is approximately given by $p(x,E_p) \approx 1 - x/R(E_p)$, where R is the range as defined by Bruining [1]. Equation (2) indicates the importance of scattering of primaries.

5. Losses are essentially constant over an entire range, *i.e.*

$$dE_p/dx\,|_{effective} = -E_p/R(E_p). \tag{3}$$

Lye and Dekker show that a generalized function of SEY can be derived using these assumptions, given by

$$\delta/\delta_m = \frac{1}{g_n(z_m)}\, g_n\left(z_m\, E_p/E_m\right), \tag{4}$$

where the function $g_n(z)$ is defined as

$$g_n(z) = \frac{1-\exp\left(-z^{n+1}\right)}{z^n} \tag{5}$$

and z_m represents that value of z for which $g_n(z)$ reaches its maximum value. A value of $n = 0.35$ was found to fit well with experimental data and was thus adopted for most materials.

Dionne was motivated to provide a physical interpretation of the variables arising in the formula for the reduced yield curve. In addition to assumptions 1-3 made by Lye and Dekker, Dionne assumes the effective escape probability for a secondary electron that reaches the surface is given by B.

The SEY $\delta(E_p)$ is derived using Eq. (1) as

$$\delta(E_p) = B \times \frac{E_p}{\Omega R} \times \left(1 - e^{-\alpha R}\right) \Big/ \alpha \,, \tag{6}$$

where Ω is the energy required to produce one secondary electron and α and R were defined earlier.

When also accounting for scattering of secondary electrons, Dionne [10] arrives at the following expressions for δ and the first cross-over energy E_1

$$\delta = \frac{B}{\zeta}\left(\frac{An}{\alpha}\right)^{1/n} (\alpha d)^{1/n-1}\left(1 - e^{-\alpha d}\right), \tag{7}$$

where

B = the escape probability,
ζ = the secondary electron excitation energy,
α = the secondary electron absorption constant,
A = the primary electron absorption constant,
d = the maximum penetration depth,
n = the power law exponent, and

$$E_1 = 0.51 E_m \delta_m^{-1.32} \,. \tag{8}$$

Note that Eq. (8) is valid only for $\delta_m > 2.5$ [10].

The important conclusions reached in [10] are summarized below:

$A \propto$ the physical density of the solid (ρ),
$\alpha \propto$ the electrical conductivity,
$B \propto 1 - r$, where r is a quantum mechanical reflection coefficient that may depend on the physical condition of the surface,
$\zeta \propto \varphi$ is the work function of the metal, and $\propto \chi + E_g$, which are the electron affinity and band gap for insulators or semiconductors.

Vaughan proposed purely empirical formulas for SEY in [11] which require prior knowledge of δ_m and E_m. These formulas incorporate the observation of angular independence at lower

energies $(\leq 0.5E_m)$. More accurate experiments at normal and oblique angles of incidence by Shih and Hor [12] involving cleaner samples led Vaughan to modify his initially proposed formulas. The modified formulas as given in [6] are

$$E_m(\theta) = E_m(0)\left(1 + {k_{sv}\theta^2}/{2\pi}\right) \text{ and} \tag{9}$$

$$\delta_m(\theta) = \delta_m(0)\left(1 + {k_{s\delta}\theta^2}/{2\pi}\right), \tag{10}$$

where k_{sv} and $k_{s\delta}$ are separate "smoothness factors" for E and δ, respectively. Both vary from 0.0 for very rough surfaces to 2.0 for very smooth surfaces with a default value of unity. Furthermore,

$$\frac{\delta(\theta)}{\delta_m(\theta)} = \left(ve^{1-v}\right)^k, \tag{11}$$

$$k = k_1 = 0.56 \forall v < 1, \tag{12}$$

$$k = k_2 = 0.25 \forall v \text{ such that } 1 < v \leq 3.6, \tag{13}$$

$$\frac{\delta(\theta)}{\delta_m(\theta)} = \frac{1.125}{v^{0.35}} \forall v > 3.6, \text{ with} \tag{14}$$

$$v = \frac{E_p - E_0}{E_m(\theta) - E_0}, \tag{15}$$

where E_0 is the minimum impact voltage at which any secondaries are generated, taken as 12.5 V; E_p is the impact voltage, and θ is the impact direction relative to the surface normal (in radians). Though empirical, Vaughan's formulas lend themselves to computer simulations and as such are used extensively in simulations involving secondary electron emission (see, *e.g.*, [13]).

III. SUMMARY OF EXPERIMENTS

The measurement techniques used here were originally proposed by Henrich [14]. A schematic of the measurement method is shown in Fig. 2.

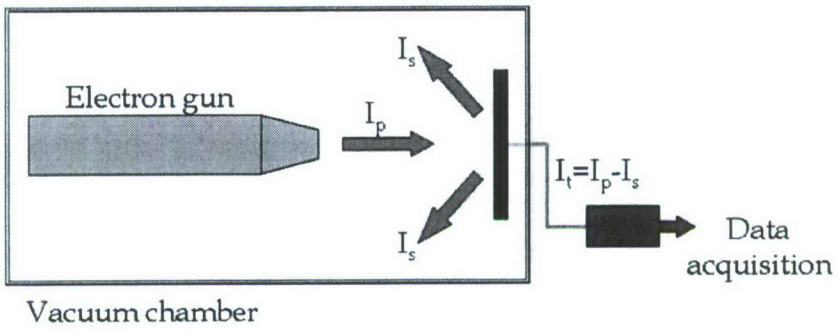

Figure 2. Measurement method to determine primary and secondary electron currents (from [5]).

The primary or beam current[1] I_p is the current emitted by the electron gun that is incident on the sample surface. This current may be determined using a device, such as a Faraday cup, whose inner surface is coated with a low yield material. A positive bias voltage on the Faraday cup (typically greater than +100 V with respect to system ground) absorbs all incoming primaries and any secondaries that may be emitted. This current denotes the total current in the absence of secondary electron emission. To determine the emitted secondary electron current I_s, a sample is placed in the path of the electron beam. For a given primary current the output or target current I_t, is less than I_p by the number of secondaries emitted by the sample, *i.e.*, $I_t = I_p - I_s$. Using the convention that electron current is positive, the total SEY is defined as [14]

$$\delta = \frac{I_s}{I_p}. \tag{16}$$

Experimentally, I_t is more easily measured than I_s. In terms of the target current, SEY can be expressed as

$$\delta = 1 - \frac{I_t}{I_p}. \tag{17}$$

Equation (17) was used to calculate δ in our experiments.[2]

[1] The terms primary current and beam current will be used interchangeably.

[2] It is important to note that the above definition does not differentiate between true secondaries and scattered primaries, as is the case with all experimental results presented in this paper.

If the sample under investigation is a metal, *i.e.,* a material with high conductivity, the beam current may be determined using the sample itself (rather than the Faraday cup) by applying a positive bias voltage on it. The utilization of the sample to measure both beam and target currents enables complete automation of the experiment. Now, the beam current is determined by application of a bias of $+V$ volts (say) to the sample. This bias will result in an acceleration of primary electrons. The net energy of primary electrons striking the sample surface will be $E_p + V$ volts. One may question whether the SEY subsequently measured corresponds to a primary energy of E_p volts (as desired) or $E_p + V$ volts. Note, however, that the beam current is set by the electron gun and not by the bias on the sample. Therefore, the number of electrons striking a biased sample (n_p and hence I_p) is constant regardless of the magnitude of the bias. The target current is determined by using an unbiased sample. In such a case, the energy of the primary electrons striking the sample surface is E_p. The output n_t corresponds to $n_p - n_s$, where n_s is the number of secondary electrons. n_p is known from the biased sample experiment, and therefore n_s can be determined for an incident primary energy E_p volts.

An overview of the experimental setup follows the block diagram shown in Fig. 3. A constant vacuum of approximately $3.9 - 5.9 \times 10^{-8}$ Torr was maintained throughout all of the experiments. In the ultra high vaccuum (UHV) stainless steel chamber (Fig. 4), a low energy ELG-2 electron gun from Kimball physics [15] was used as the electron source. The gun has an energy range of 5 eV-1000 eV, beam current range 10 nA-10 μA and average spot size of 0.38 mm at an optimum (manufacture-specified) operating distance of 20 mm. A custom designed sample holder was used to ensure optimal operating distances. The linear and angular manipulators enabled horizontal translation and rotation of the sample. In a few experiments the thermocouple was used to monitor the temperature on the sample surface, while a quartz lamp heater was used to heat the sample to approximately 100-300 Celsius.

The sample bias switch was used to bias the sample negative (usually to approximately -20 V) while measuring the target current in some experiments (results of these experiments are also not presented). The relay trigger and battery bank comprised the automation system. The battery bank is simply an array of batteries used to achieve a voltage between 0-500 V DC and was used to bias the sample positive during beam current measurements. Two double-pole-double-throw (DPDT) latching relays were used to switch between measurement of beam and target currents (Fig. 5). This has the advantage of eliminating beam drifts as beam and target current measurements are taken with minimal time delay at the same energy.

A Keithly electrometer [16] capable of measuring currents from a few pico-amperes to 21 mA was used (currents in our experiments varied from approximately $10^{-7} - 3 \times 10^{-5}$ A. A diode protection circuit was used as an extra buffer that prevented damage to the electrometer in case too much current was sourced by the battery bank (Fig. 6, with $R = 10\,\mathrm{k}\Omega$). The data acquisition system used a customized LabView program to adjust various desired parameters in the system and acquire beam and target current data.

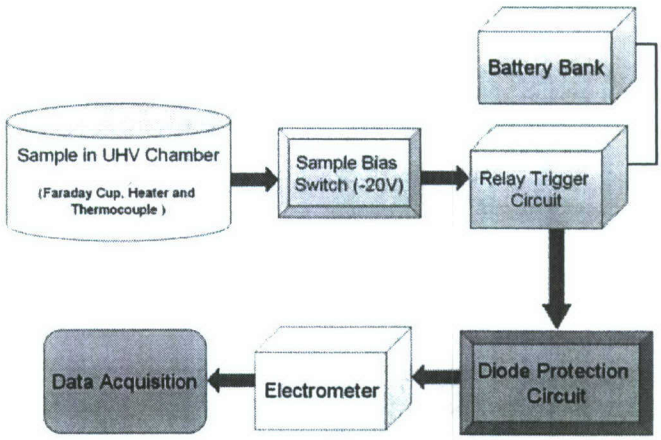

Figure 3. Schematic of the experimental set-up.

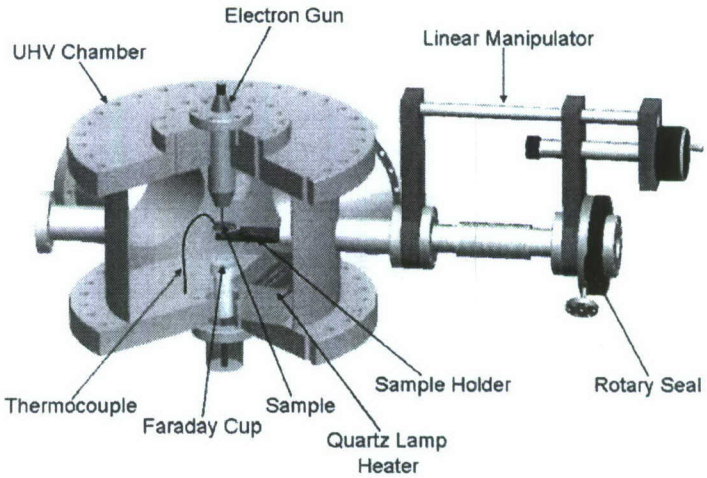

Figure 4. Schematic of the UHV chamber used for SEY measurements.

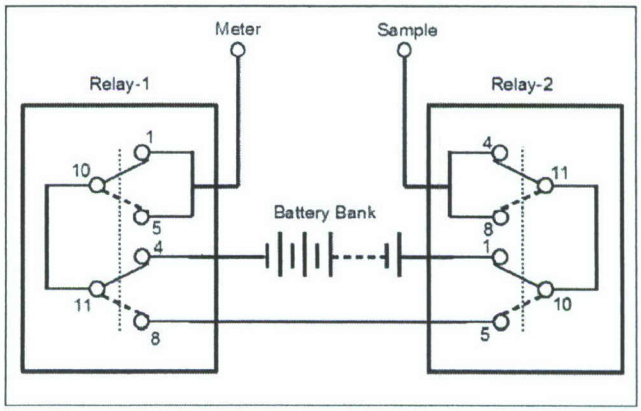

Figure 5. Equivalent circuit of the relay trigger.

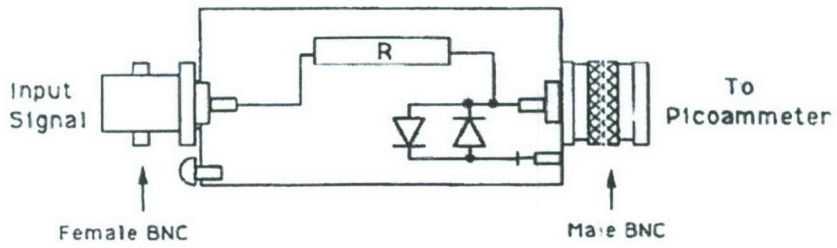

Figure 6. Schematic of the diode protection circuit.

A. TERMINOLOGY

The SEY δ is calculated using Eq. (17). Electron dose D is defined as the total charge incident per unit area on the sample surface when measuring SEY. The units of dose are C/mm^2. Current density J is a vector quantity whose magnitude is the ratio of the magnitude of beam current to the cross-sectional sample surface area perpendicular to current flow and whose direction points in the direction of the beam current. The units used here are A/. Note that current density may also be considered as the dose per unit time i.e. $C/mm^2/s$. The area simply introduces a proportionality factor since it is constant in our experiments. Therefore, area is neglected while comparing similar results and only beam current is stated in such cases. Dose information is easily obtained from current density by integrating over the time period for which the surface was exposed for each data point. Where necessary, specific mention is made as to whether dose or current density is considered. For oblique angles of incidence for primary electrons, angle is referenced with respect to surface normal, as is conventional in SEE theory.

B. SUMMARY OF EXPERIMENTAL PARAMETERS

The operating distance between the electron gun and sample surface that was used was 40 mm instead of 20 mm to reduce beam current density incident on the sample surface (increasing the distance moves the sample from the beam focus, this increases the incident beam diameter).

Most experiments were performed by scanning beam energy from lowest to highest energy value while measuring SEY at each energy. As will be seen later, changes in this procedure affect yield significantly. For each beam energy, first the beam and then the target current data points were acquired by averaging 500 measurements at 0.2 seconds/measurement for each data point. This resulted in a total exposure time of 200 seconds per data point (100 seconds for beam current and 100 seconds for target current). However, only the duration of beam current in the unbiased sample experiment is considered for calculation of electron dose. Since no SEE takes place in the biased sample experiment, this duration is not considered. Therefore for the above case, I_p for 100 seconds for each data point is

considered. Ideally one would consider both beam and target currents, since both these currents cause surface modifications. Inclusion of beam current in our experimental data would simply introduce a proportionality factor and, as such, would not affect the conclusions reached.

The electron beam was normal to the sample surface. The sample was biased at approximately +150 V during measurement of I_p. Pressure was maintained at approximately 5×10^{-8} Torr. Unless explicitly mentioned, the parameters stated above are to be assumed as the default in all experiments.

IV. SUMMARY OF SAMPLES AND PREPARATION PROTOCOLS

Recently, most experiments described in the literature have shifted focus from "pure metals" to "technical materials" (for a definition of "technical materials" see [2,4]). Technical materials are, in general, pure materials with contaminants on the surface (generally oxides, water vapor, and adsorbed particles). Such a shift has arisen from the need to obtain results for practical applications. Results presented here include both pure and technical materials.

Three different metals were tested:

1. Copper (Cu),
2. Plasma-sprayed boron carbide (PSBC) on a copper substrate, and
3. Titanium nitride (TiN) on a copper substrate.

Copper was primarily used for benchmarking purposes, as a result of which it was subject to the largest amount of study. Extensive data in the literature on copper involving varying doses, surface conditions, and angles of incidence (see, *e.g.,* references cited in [1-4]) made it a convenient material for purposes of comparison. Two different copper samples were used. The first copper sample (Cu-1) was provided by Calabazas Creek[3]. The second copper sample (Cu-2), tested previously in our laboratory [5] was used due to suspicions that results may have been influenced by surface modifications to the first sample.

Experiments on Cu-1 were conducted for two different surface conditions/treatments: 1) as-received atmosphere-exposed and 2) argon glow-discharge (AGD) cleaned. Experiments on Cu-2 were performed after AGD cleaning the surface.

Plasma sprayed boron carbide was also provided by Calabazas Creek as part of an ongoing investigation to identify low yield materials for use in collectors of microwave tubes. The sample consisted of plasma sprayed boron carbide of thickness approximately 127 μm on a copper substrate. Experimental results for PSBC are significant as SEY curves for this sample have not been previously published. Many experiments conducted on copper were extended to PSBC to determine the nature of yield curves under corresponding experimental conditions. PSBC was subjected to methanol andAGD cleaning, although prolonged AGD cleaning resulted in the formation of a highly carbonaceous layer along the edges of the sample surface.

Titanium nitride was provided by CPI[4]. The sample consisted of a few10's nm-thick layer of TiN on a copper substrate. The sample was not exposed to air for longer than (approximately) 20-30 minutes and the surface was not treated with alcohol. TiN was not

---

[3] Dr. Lawrence Ives, Calabazas Creek Research, Inc., 690 Port Drive , San Mateo, CA 94404-1010, USA (http://calcreek.com/).

[4] William C. Guss, Communications and Power Industries, Inc., Beverly Microwave Division, 150 Sohier Road Beverly, MA 01915-5595, USA (http://www.cpii.com/division.cfm/8).

AGD cleaned in fear of damaging the extremely thin layers.

It should be noted that all samples consisted of thin layers of the respective substance over a copper substrate. This fact may be of relevance in regard to the coefficient "A" in Dionne's theory.

The AGD was achieved by using a neon transformer with rated output of 12 kV/30 mA. The chamber was filled with argon (100-500 mTorr fill) and an argon plasma was formed. The sample surface and a thin copper plate mounted on the Faraday cup were used as electrodes (see Fig. 4). A negative bias of the order of -100 V was applied to the sample to ensure efficient cleaning by ions.

As regards the chemical nature of surfaces prior to AGD cleaning, it was impossible to avoid the formation of monolayers as samples were inserted manually into the chamber after being exposed to air, although care was taken to minimize exposure time. An AGD presumably cleaned the surfaces of samples by removing monolayers; nevertheless, none of the samples may be considered clean to degrees achieved by [12 and 14]. Typical monolayer formation time for the nominal base pressure was estimated to be on the order of one minute.

As for surface morphology, the samples in order of decreasing surface roughness (by visual observation) are as follows: PSBC (roughest), Cu, and TiN (smoothest).

V. SUMMARY OF EXPERIMENTAL OBSERVATIONS

Results presented here are broadly divided into four categories:

1. Dose effect,
2. Influence of surface conditions on the dose effect ,
3. Temporal behavior of SEY, and
4. Dependence of SEY on the angle of incidence of primary electrons.

It should be noted that the largest percentage error in measurements was due to uncertainty in the target current. However, a preliminary error analysis indicates an error in target current of the order of 1% and an overall error of less than 5%. Therefore, the error bars in all results presented here are the same order of magnitude as the point size.

A. THE DOSE EFFECT

This section summarizes results of the variation of the SEY with electron dose/beam current density. All data sets in all experiments were taken on a fresh spot.

Yield curves obtained for SEY versus incident beam energy for the AGD cleaned copper (Cu-2) sample for several current densities are shown in Fig. 7. The overall shape of the curves mimic the generic curve of Fig. 1. However, the dose effect is clearly observed in this figure, *i.e.,* the SEY decreases with increasing electron dose (current density) for a fixed primary energy.

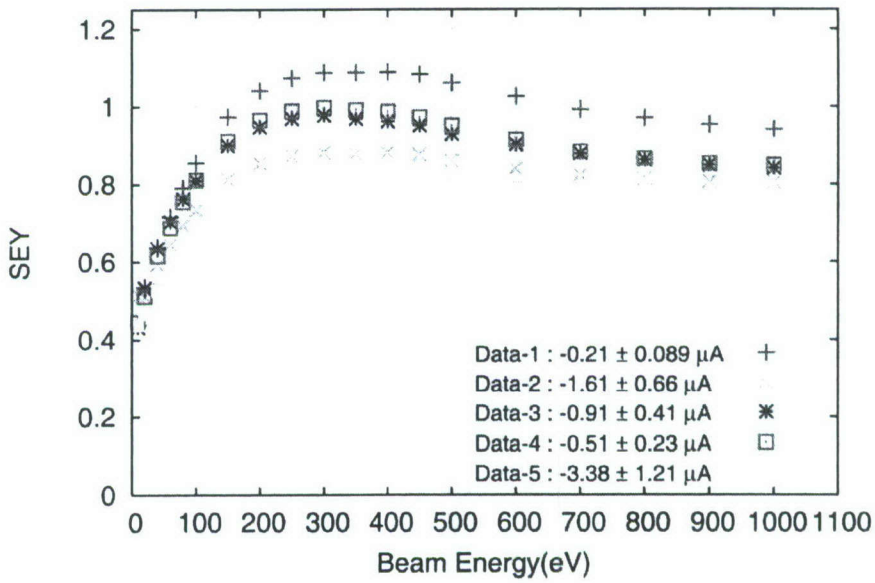

Figure 7. SEY curves for Cu-2 are in agreement with Baglin *et al.*'s results [2]. The notation Y ± XX indicates average beam current (Y) with standard deviation (XX).

Similar results were obtained for PSBC and TiN and are shown in Figs. 8 and 9. Note again the consistent decrease in SEY with increasing current density for both PSBC and TiN.

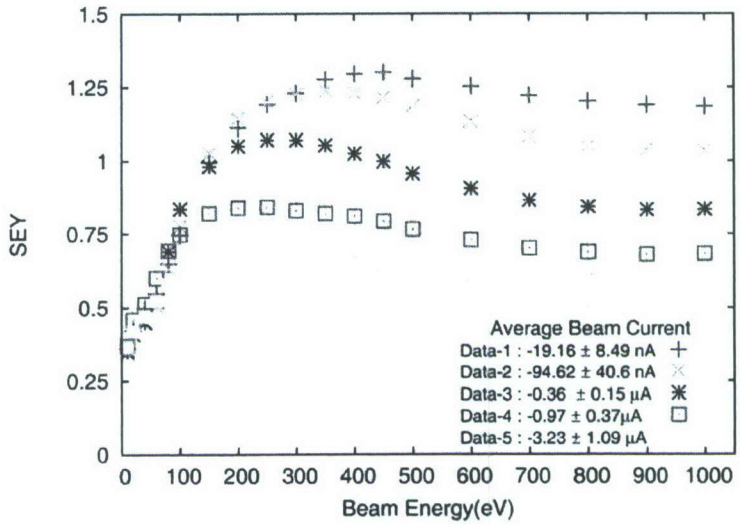

Figure 8. Variation of SEY with current density for PSBC.

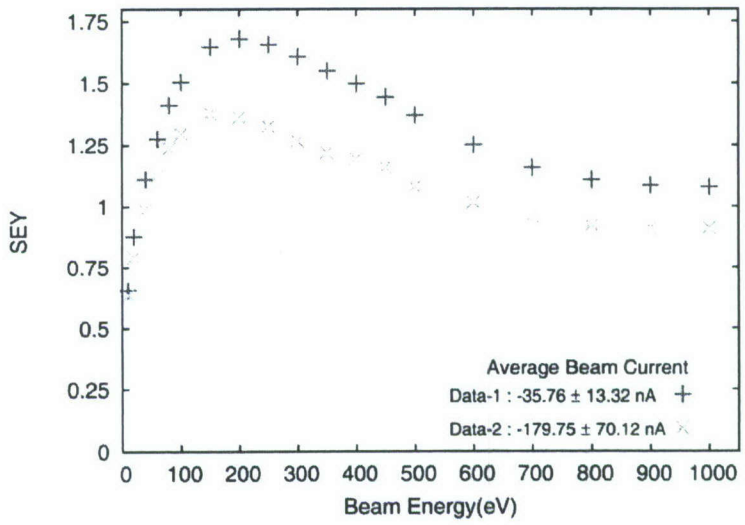

Figure 9. Variation of SEY with current density for TiN.

While PSBC was AGD cleaned, TiN was used as-received. It is therefore highly likely that the SEY obtained for TiN are a convoluted result of surface contaminants (such as TiO_2) with pure TiN.

The maximum energy in all cases is found to shift with increasing electron dose. This shift, generally unpredictable, is believed to be a consequence of surface contamination and will be discussed in a later section of this report.

Yield curves were independent of dose below the minimum and above the maximum current densities indicated in Figs. 7 and 8. It may be concluded that there exists a minimum dose D_L and a maximum dose D_H between which the SEY of a substance is bounded, *i.e.,* the yield is independent of dose below D_L and above D_H. Note also that the independence of yield above D_H may be one of the factors responsible for saturation observed in two-surface multipactors [17].

In the most simplified case, the dose effect makes the following statement: Let D_1, D_2 be two doses and δ_1, δ_2 be their corresponding SEY. If $D_1 > D_2$ for a fixed primary energy, then $\delta_1 < \delta_2$. Practically, however, the results obtained are very sensitive to the surface conditions of the samples being investigated. The effects of surface contamination on SEY in the context of the dose effect are discussed in the next section.

The Cumulative Nature of the Dose Effect

The definition of electron dose in the context of SEY turns out to be counter-intuitive. Consider the following argument: In all results presented in this report the SEY are obtained for discrete energies and doses. Consider, then, yields $(\delta_1, \delta_2, \delta_3, ...\delta_n)$ obtained at corresponding energies $(E_1, E_2, E_3, ...E_n)$ and corresponding doses $(D_1, D_2, D_3, ...D_n)$. The continuous nature of experiments conducted here lead to an important concern: is $\delta_n \propto f(E_n, D_n)$ or $\delta_n \propto f\left(E_n, \sum_{k=0}^{n} D_n\right)$? In other words, is the electron dose considered independently for each measurement period or is a cumulative sum of doses considered for each measurement period, wherein doses from previous measurement periods are also taken into account?

Intuitively one expects $\delta_n \propto f(E_n, D_n)$. However, this is not the case as was borne out by experiments when yield data was acquired in *descending* order of beam energy. This is explained as follows: All yield data presented in this report thus far were acquired in ascending order of energy, scanning from lowest to highest primary energy to acquire each data point. In this order, less cumulative charge is received by the sample at low energies compared to higher energies, whereas in decreasing order the converse is true. If SEY were inversely proportional to the total amount of charge received over a measurement period, then in descending order, lower energies would have a lower SEY while higher energies would have a higher SEY compared to ascending order experiments. The results obtained for such "ascending-descending" experiments on as-received, air-exposed Cu-1 are shown in Fig. 10.

The cumulative nature of the dose effect is eminently clear because results obtained are exactly as expected. Using the results from above, the electron dose at a particular energy is calculated as the cumulative sum of doses incident during the measurement of earlier and present yields in the same experiment. Henceforth, electron dose will be used to refer to the

cumulative dose as described in this section.

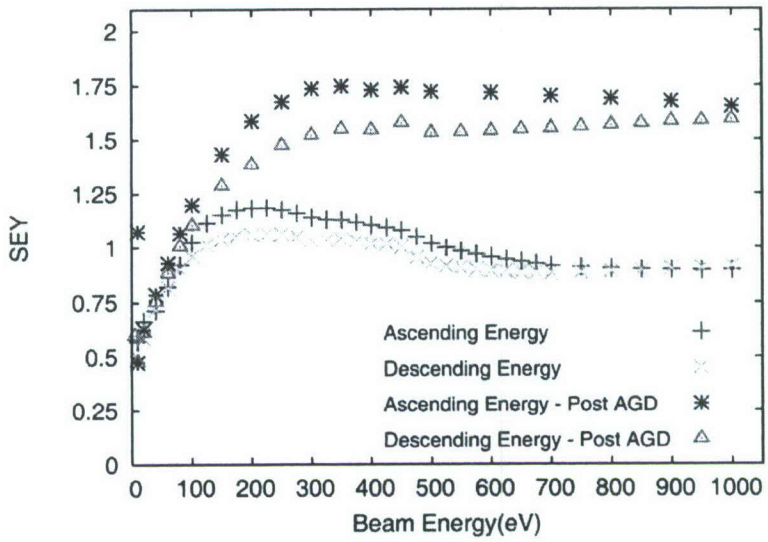

Figure 10. Variation of SEY with energy for "ascending-descending" experiments.

General Observations on the Dose Effect

Observe that in Figs. 7 and 8 the SEY decreases faster (with increasing electron dose) for lower primary energies than for higher primary energies. This fact that the dose effect is more pronounced at lower primary energies was observed by Baglin *et al.* [2]. Figure 11 presents a plot of the variation of SEY for Cu-1 versus current density. Plots of normalized SEY versus electron dose for experimental data in Figs. 7, 8, and 11 (area = 0.5mm^2) are shown in Fig. 12. Although the results obtained here do not seem to follow as smooth a trend as those obtained by Baglin *et al.*, it is observed that the dose effect is more pronounced at lower primary energies. This is not as clear for the case of PSBC as it is for Cu-1 and Cu-2.

Since the quantity δ_m is encountered so frequently in the theory of SEE, it is interesting to observe the variation of δ_m as a function of electron dose D. Such plots of SEY for Cu-1, Cu-2, and PSBC (for experimental data in Figs. 7, 8, and 11) as a function of electron dose are shown in Fig. 13. An exponential dependence of maximum yield on electron dose is observed. These curves agree very well with similar results obtained by Kirby and King [3].

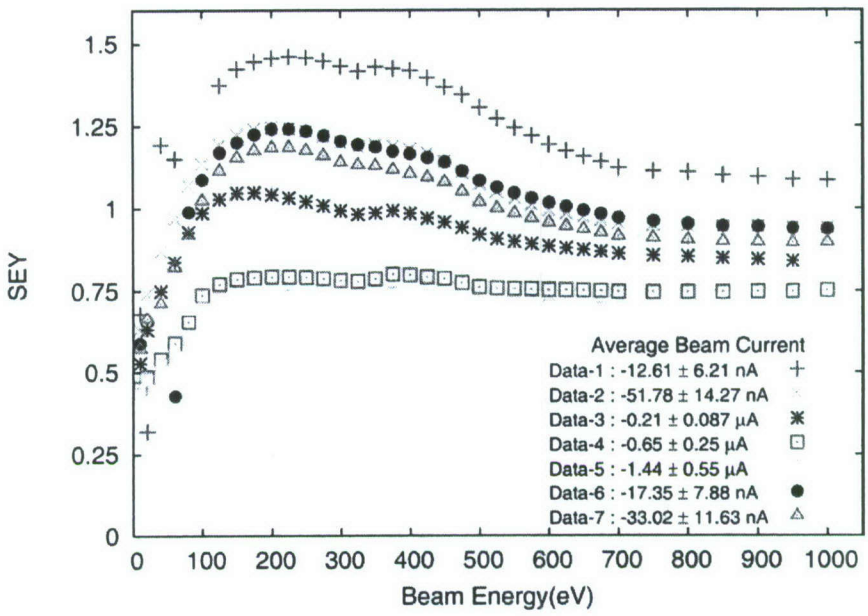

Figure 11. Variation of SEY for Cu-1 with energy for varying current density.

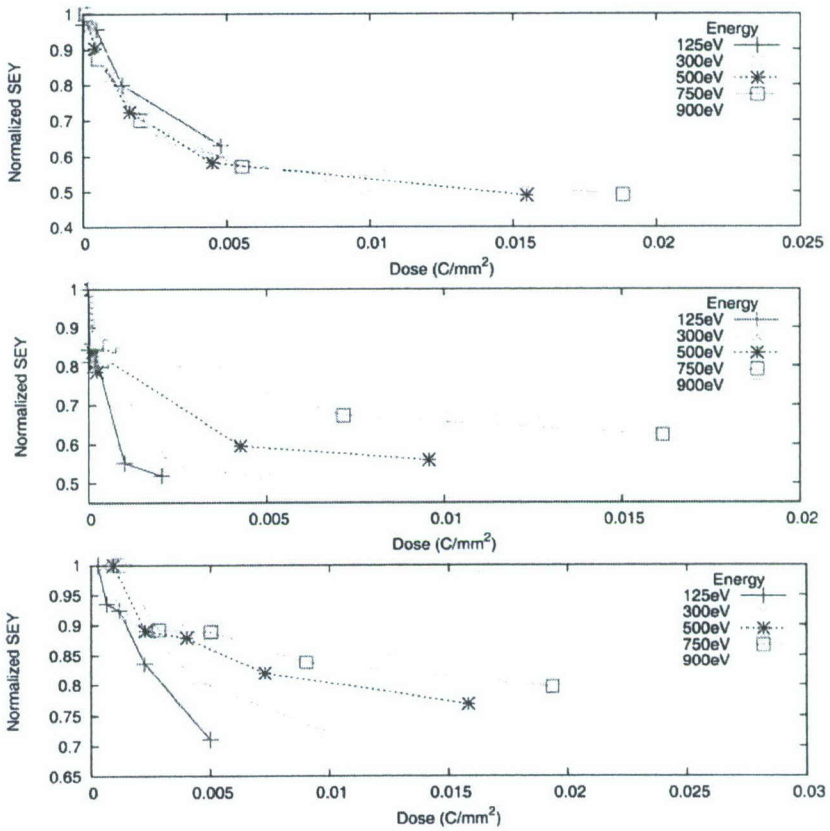

Figure 12. Dose comparison at various energies for Cu-1 (top), Cu-2 (middle), and PSBC (bottom) following AGD cleaning.

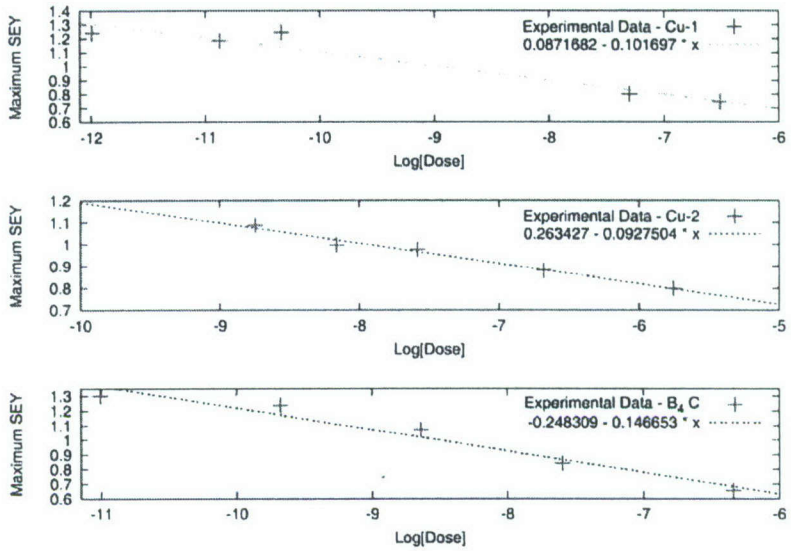

Figure 13. Peak SEY as a function of normal electron dose for Cu-1 (top), Cu-2 (middle), and PSBC (bottom).

B. THE INFLUENCE OF SURFACE CONDITIONS ON THE DOSE EFFECT

It is emphasized that the dose effect is a surface phenomenon. Physio-chemical surface conditions play a very important role and influence SEE heavily (see, for example, the references cited in [1]). Therefore, in any SEE experiment, it is important to examine and characterize the surfaces under investigation. This section aims to present results of studies of the samples' surface and the influence of surface conditions on SEY in the context of the dose effect.

Yield curves were obtained the for as-received, air-exposed copper (Cu-1) sample for several current densities and were earlier shown in Fig. 11. Two important points are to be noted from Fig. 11: Firstly, the occurrence of two maxima for a yield curve at fixed current density (for example consider Data-2) indicates deviations from the theoretical curves as well as from those published in the literature. Secondly, note that the dose effect continues to be prevalent for all current densities although the sample is unclean. The fact that the two maxima are replicated for all current densities indicates that the dose effect acts uniformly (at all energies) for given surface conditions. Changing the surface conditions may influence the shape of an individual yield curve, but the SEY will continue to decrease with increasing current density in a manner dictated by the dose effect.

In order to explain the occurrence of two maxima for an individual yield curve, the theory proposed by Kirby and King [3] is adopted. For this, the curve is divided (somewhat arbitrarily) into three regions, as is shown in Fig. 14. At low energies the electron beam is unable to penetrate the surface and reach the sample. Therefore, region I is thought to represent yield chiefly due to contaminants and adsorbed particles (probably, copper oxides and hydroxides) on the sample surface. At higher energies, *i.e.,* in region III, the

oxide/hydroxide dielectric layer is damaged and SEY is primarily due to the pure copper substrate. The SEY in region II is possibly due to both oxide/hydroxide dielectric layers and pure copper. It appears that the convolution is more complex in this case than a simple decaying exponential as observed by Kirby and King [3] in their experiments. As a possible example of yield curves that may involve convolution to produce the data similar to that shown Fig. 11, a plot of Lye and Dekker's curves which may produce the two maxima are also shown in Fig. 14. Note that a family of curves may be obtained by varying the parameter n in Lye and Dekker's formula. Any of these curves may be used to match the experimental data.

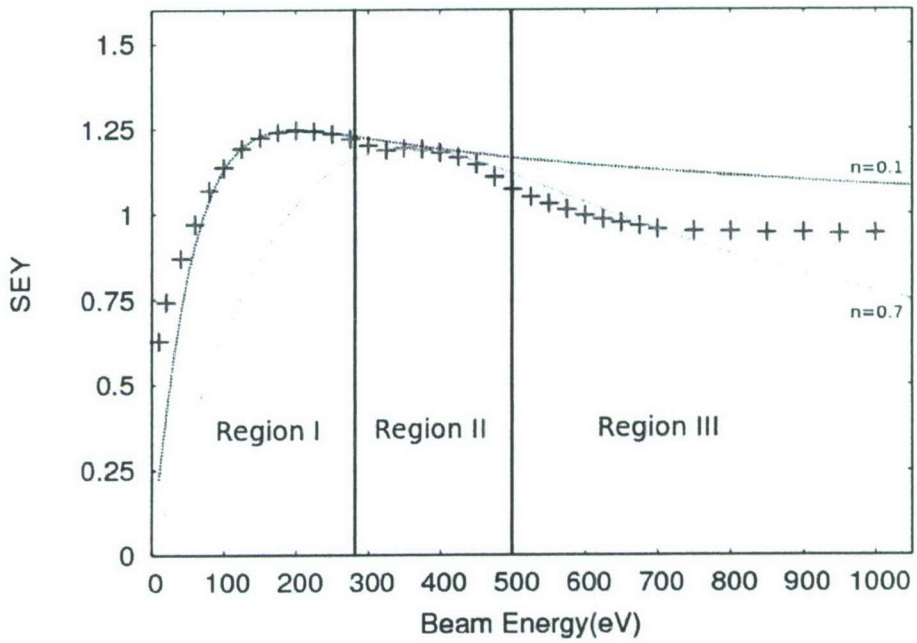

Figure 14. Experimental data (the experimental dataset is Data-2 (+) from Fig. 11) plotted against Lye and Dekker's curves for the first maximum (blue) and second maximum (green). The experimental curve is divided into three regions based on the maxima, as is discussed in the text.

The reason for the appearance of two maxima in Fig. 11 is strongly suspected to be surface contamination. The sample was therefore cleaned using a prolonged AGD plasma for 12-15 hours. This resulted in the formation of a permanent chemical layer on the sample surface which, in turn, gave rise to steep gradients in the SEY curve toward higher energies (>400 eV).

As a final attempt to produce SEY curves with minimal surface contaminants and without any surface modification, the copper sample (Cu-2) used in previous studies [5] was used. The sample surface was AGD cleaned for a relatively shorter time period, approximately 4-6 hours. The results of the variation of SEY with current density are compared with Baglin *et al.'s* [2] data in Fig. 15. Although experiments on Cu-2 were conducted at slightly higher current densities, good agreement with Baglin *et al.'s* data in terms of the shape of the curves

is observed. Note that plots in Fig. 15 are not strictly correct as comparisons are made between current density (experimental results) and electron dose (results in [2]). Nevertheless, for a given material, the *shape* of SEY curves will remain unchanged. It is this point that is emphasized.

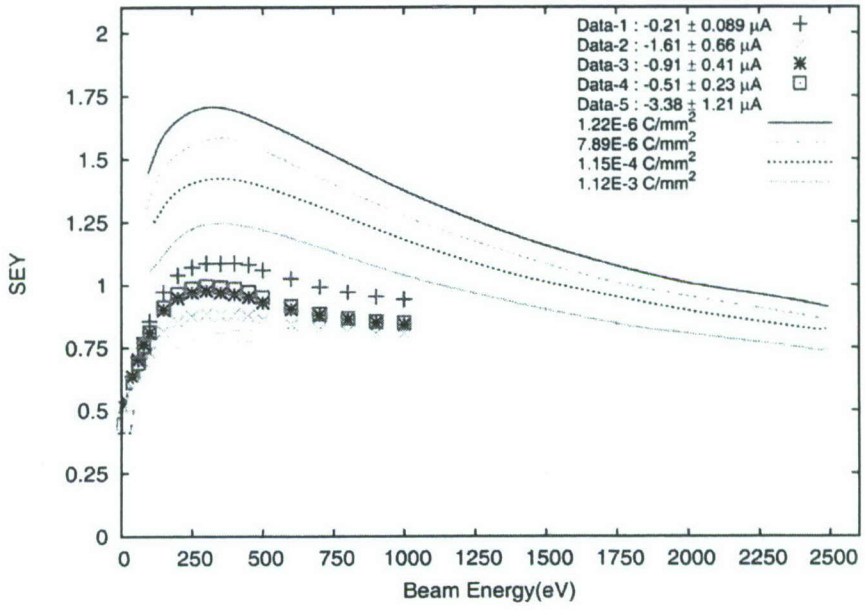

Figure 15. The shape of the SEY curve for Cu-2 is in good agreement with the results of Baglin *et al.* [2].

There may be some doubts on the experimental procedure after the realization of yields less than unity were obtained for copper at higher current densities (see, *e.g.*, Data-5 in Fig. 11). However, the results presented here seem to indicate that, for given experimental conditions, the maximum yield of copper reaches a constant value of approximately 0.6 at greatest dose. The use of such high doses have not been found to be documented elsewhere. The critical issue is, of course, how these doses would compare with the actual environment in the collector of an HPM sources.

C. TEMPORAL VARIATIONS IN SEY

As the electron dose increases, the SEY decreases for fixed primary energy. However, at higher current densities it is believed that another important phenomenon may be primarily responsible for causing deviations – beam-induced surface reactions. Beam-induced surface reactions lead one to expect temporal variations in SEY because surface compounds formed would in turn affect the yield. This process would take place until some equilibrium is reached. In contrast, the lack of beam-induced reactions at lower current densities implies a relatively constant SEY with time. This section presents results of SEY as a function of time. The literature on temporal variation of SEY is sparse and provides very little explanation as to the cause of variations.

The temporal dependence of SEY at 100 eV and 1000 eV with low and high current densities for AGD cleaned Cu-1 is shown in Fig. 16 where SEY (normalized with respect to its maximum) is plotted versus time. Temporal variations at other energies are summarized in Table 1.[5]

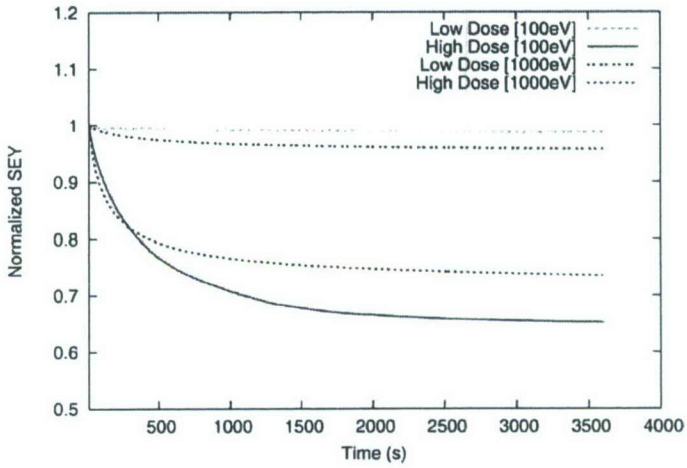

Figure 16. The variation of SEY with time for high and low dose at 100 eV and 100 eV primary energies.

TABLE 1. Relative variations in SEY as a function of time over approximately 1 hour for low and high current density (J) beams at a given beam energy.

BEAM ENERGY	% VARIATION IN SEY FOR LARGE J	% VARIATION IN SEY FOR LOW J
100	34.79	1.31
250	10.14	4.71
450	10.60	3.21
700	21.13	9.36
1000	26.49	4.29

Although not as long duration as the experiments of Lavarec [4], Table 1 clearly shows that the percentage variation in SEY with high current density is much greater than the percentage variation in SEY with low current density at a given energy. These results are consistent with those obtained by Lavarec. For a perfectly clean sample, the cumulative nature of the dose effect leads one to expect

$$\delta(E, D_L)|_{t=t_1} \approx \delta(E, D_H)|_{t=t_2}. \tag{18}$$

Unfortunately, such a comparison could not be performed for the data in Table 1 as there were no common cumulative doses between two curves at the same primary energy of electrons.

[5] The precise definitions of the terms "high" and "low" are given in a later section of this report based on results presented in this section

That beam-induced surface reactions at higher current densities (or equivalently, after prolonged exposure to the electron beam) is likely the primary cause is evident from the photographs of the copper and boron carbide samples shown in Fig. 17. Note the discoloration at point of impact of the electron beam.

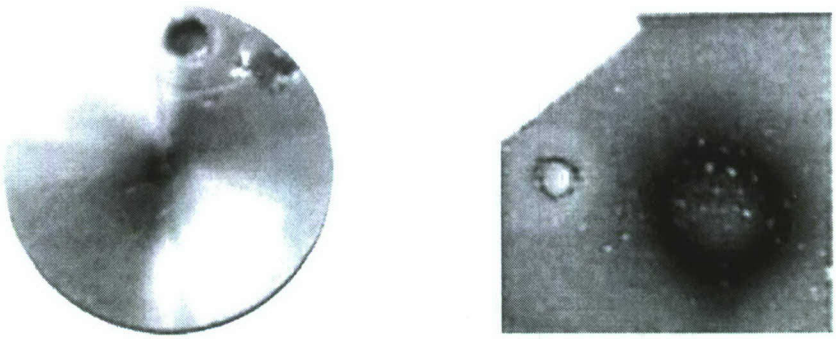

Figure 17. Photographs of the copper sample (left) and the PSBC (right) following prolonged exposure to the primary electrons. Note the discoloration at the point of impact.

The contamination on the sample surface in these cases is due to oxides and hydroxides of carbon. Figures 18-21 present XPS analysis of these samples. Observations of carbonaceous compounds through more extensive analysis have been documented throughout the literature (see, *e.g.,* references in [1, 3, and 18]. It is possible that the carbon required for forming the spots in Fig. 17 came from within the material itself (as proposed by Henrist *et al.* [18] or were the result of adsorption from residual gases in the chamber. From the photographs it appears that beam-induced carbon and hydrocarbon formation occurs when a sample is exposed to high current densities for an extended period of time. It is not possible to determine whether a higher or lower yield was responsible for a compound formed on the surface. It is clear, however, that there are marked differences between high and low current density experiments for the same sample under similar experimental conditions.

Perhaps the most significant implication of observations in this section is in regard to the work done and conclusions reached by Zameroski in [5]. Extensive experiments were conducted to investigate the time varying SEY (albeit at much higher beam energies) and the subsequent discoloration of the samples used. The observations in [5] are consistent with the results presented here and with those of Lavarec *et al.* [4]. It seems reasonable to conclude that the experiments in [5] were beyond the "critical point" described by Lavarec, *i.e.,* these experiments were conducted in a regime of current densities which catalyzed carbon formation and other surface chemical reactions. Thus, Zameroski's observations appear to be a direct consequence of the dose effect.

Sample 1, low resolution survey

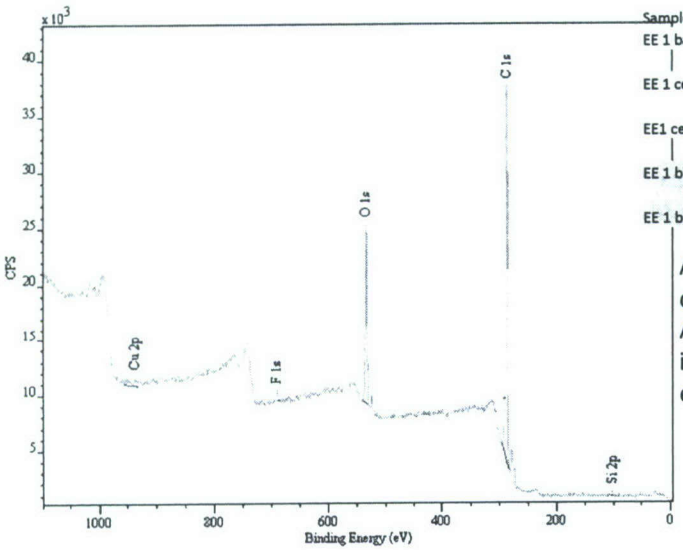

Sample Identifier	Cu 2p %	O 1s %	C 1s %	F 1s %	Si 2p %
EE 1 back	0.4	18.0	80.2	0.5	0.9
EE 1 center 1	0.5	17.5	80.5	0.8	0.7
EE1 center 2					
EE 1 black edge	0.4	15.7	81.7	1.4	0.7
EE 1 black edge	0.2	18.2	79.7	0.7	1.2

Almost no Cu is detected. All covered in C.
Almost no difference in areas inside dark areas and darkest edge and background.

Figure 18. Low resolution XPS analysis of the PSBC sample shown in Fig. 17.

Sample 1, High resolution C

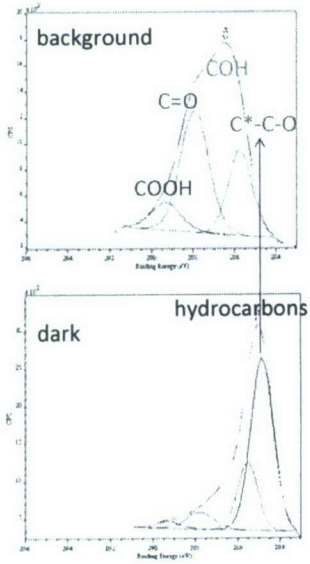

	C 1s deconvolution				
	C-C (hydro-carbons)	C*-C-O	C-OC, C-OH	C=O	COOH
Sample Identifier	*284.9*	*285.5*	*286.5*	*287.9*	*289.3*
EE 1 back		20.0	38.9	33.2	7.9
EE 1 center 1	58.1	17.8	13.3	7.7	3.0
EE1 center 2	55.4	20.1	14.6	7.2	2.8
EE 1 edge	46.2	27.3	15.0	7.2	4.3

Dark areas are rich in hydrocarbons They are absent at all in background area. Even though the same amount of C is detected for background area, they are mostly – CxOy species.
Dark areas are 50% HC and 50% CxOy species

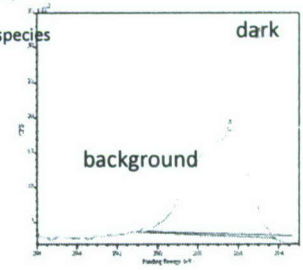

Figure 19. High resolution XPS analysis of the PSBC sample shown in Fig. 17.

Sample 2, low resolution survey

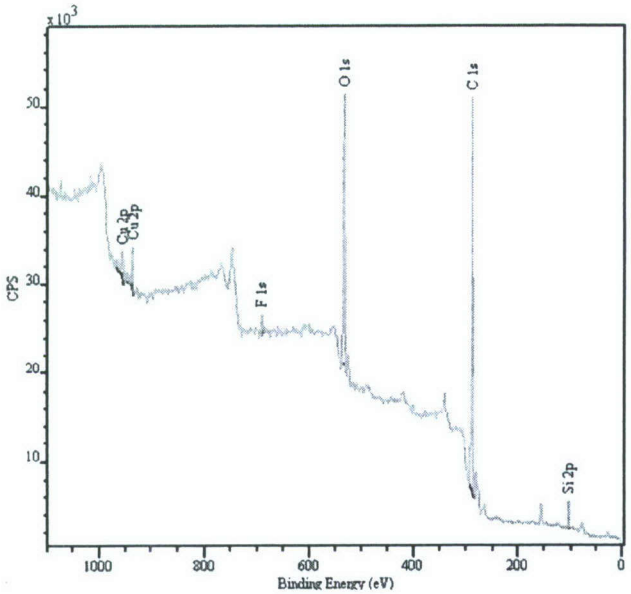

	Cu 2p %	O 1s %	C 1s %	F 1s %	Si 2p %
EE 2 back	1.7	20.8	72.5	1.3	3.7
EE 2 black 1	0.8	22.6	70.6	1.6	4.3
EE 2 black 2	0.9	22.5	70.5	1.6	4.5

More Cu is detected. All covered in C.
Slightly less Cu and more Si in dark areas.

Figure 20. Low resolution XPS analysis of the copper sample shown in Fig. 17.

Sample 2, high resolution C

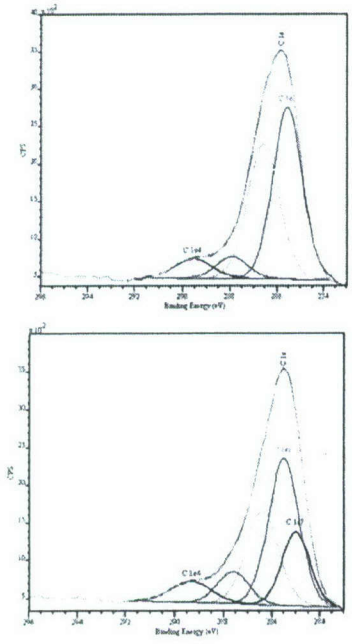

	C 1s deconvolution				
	C-C (hydro-carbons)	C*-C-O	C-OC, C-OH	C=O	COOH
	284.9	*285.5*	*286.5*	*287.8*	*289.3*
EE 2 back		46.4	40.0	6.6	7.0
EE 2 black 1	18.9	39.1	26.9	7.6	7.7
EE 2 black 2	17.9	39.1	26.7	8.9	7.5

Less pronounced differences that for 1st sample.
Only 20% of HC is present for dark areas comparatively with background.

Figure 21. High resolution XPS analysis of the copper sample shown in Fig. 17.

D. VARIATION OF SEY WITH THE ANGLE OF INCIDENCE OF PRIMARY ELECTRONS

The results presented in this section are not related to dose dependence, but rather were performed to confirm theoretical predictions and compare our experimental data with those found in the literature. The SEY as a function of the angle of incidence of primary electrons is shown in Figs. 22 and 23 for AGD cleaned PSBC and Cu-2 samples, respectively. Note that the results obtained are *not*, generally speaking, in very good agreement with Vaughan's formulas (see, *e.g.,* [12]). In particular, increase in the SEY of copper is greater with increasing angle of incidence, in contradiction with Vaughan's formulas. The results for the SEY of PSBC, however, show better agreement with Vaughan's formulas. Note that at low energy (<100 eV) the independence of SEY on angle *is* observed in Figs. 22 and 23.

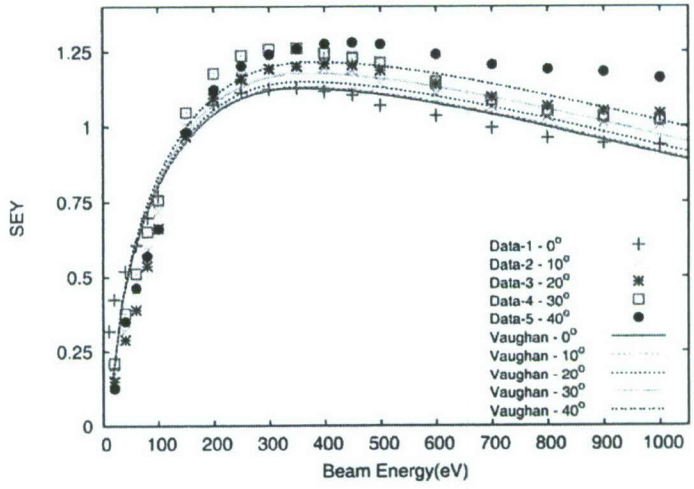

Figure 22. Comparison of the dependence of the SEY on AGD cleaned PSBC as a function of angle of incidence with Vaughan's formula.

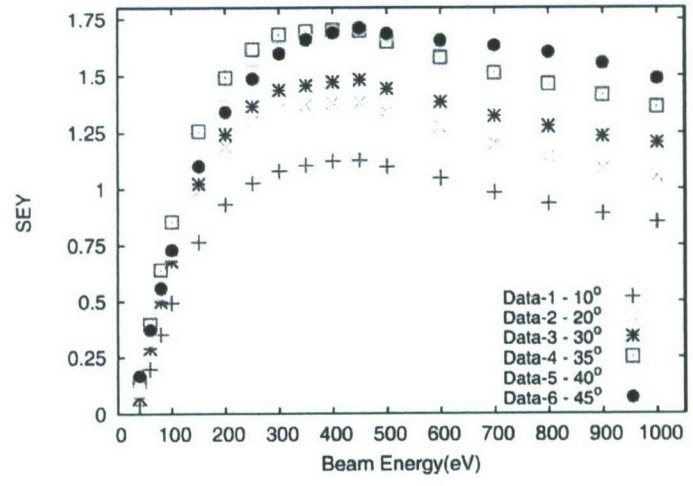

Figure 23. Comparison of the dependence of the SEY for Cu-2 as a function of angle of incidence with Vaughan's formula.

Curve fits shown in Fig. 24 seem to re-affirm Kirby and King's [3] conclusions as the normalized maximum yields (*i.e.* yields normalized with respect to maximum yield at normal incidence) fit better to an exponential dependence (as explained by Bruining [1]) as opposed to a $1/\cos\theta$ variation. It is suggested that this may not be a phenomenon that is only surface-related.

The exact nature of changes in SEY with respect to the primary electron's angle of incidence *and* varying dose is a subject of further investigation. It is possible there is a dependence of the rate of change of SEY on electron dose and angle of incidence.

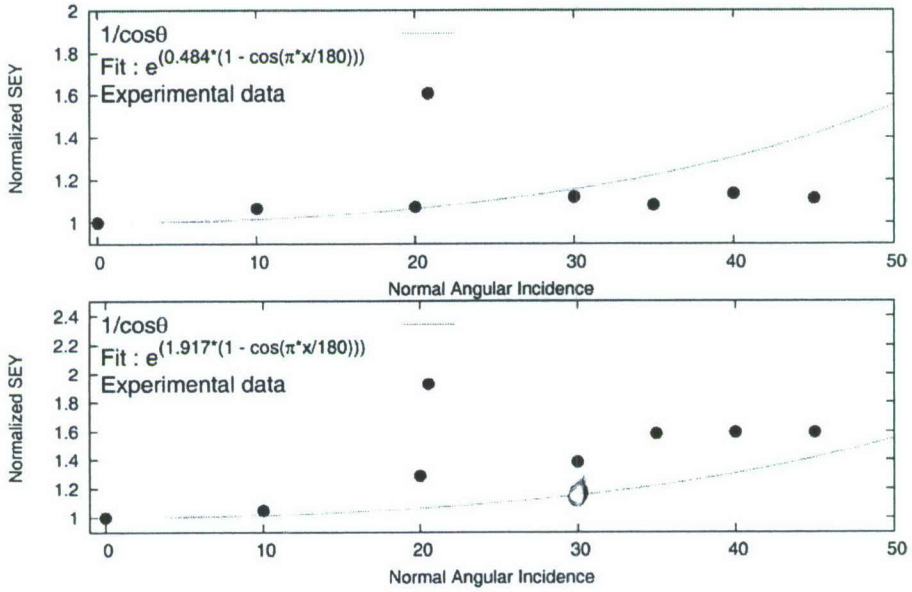

Figure 24. Normalized peak yields versus the primary electron's angle of incidence for PSBC (top) and Cu-2 (bottom).

VI. THEORETICAL DISCUSSIONS

Based on the results discussed in the preceding sections, this section attempts to formulate empirical relationships of dose and angular dependence on SEY, which are later incorporated into the Vaughan and Lye and Dekker formulas.

One may begin by considering observations in Fig. 13 and Kirby's [3] results where maximum yield was linearly related to $\ln|D|$. For this linear relationship to be physically valid, the logarithmic argument must be dimensionless. In order to accomplish this, the equation $y = mx + b$ may be modified as $y = mx + \ln|p| = m\ln|pz|$ so as a first approximation, maximum yield at normal incidence may be related to dose by Eq. (19)

$$\delta_m(0) = m\ln|pD|, \tag{19}$$

Where m (dimensionless) and p (mm^2/C) are constants. In general m, p, and D may be functions of the primary electron energy and angle of incidence.

The phenomenological theory proposed by Bruining [1] provides better agreement for the dependence on angle of incidence, as is observed from results obtained here and those obtained by Kirby and King [3]. Based on this, the SEY at oblique angles of incidence may be related to SEY at normal incidence as

$$\delta_\theta = \delta_0 e^{\alpha X_m(1-\cos\theta)}, \tag{20}$$

where δ_0 is the SEY at normal incidence, α is the absorption coefficient, and X_m is the average depth at which N secondary electrons are generated at normal incidence.

If the reduced SEY curve at normal incidence is given by function f such that

$$\frac{\delta(0)}{\delta_m(0)} = f \Rightarrow \delta(0) = f\delta_m(0), \tag{21}$$

then, using Eq. (19), we obtain

$$\delta(0) = fm\ln|pD|. \tag{22}$$

Hence, a generalized expression for δ as a function of the angle of incidence of primary electrons and dose can be written as

$$\delta(\theta) = fm\ln|pd|e^{\xi(1-\cos\theta)} \tag{23}$$

with $\xi = \alpha X_m$.

It is clear that none of the previously proposed theories take into account modifications due to the dose effect. Using the relation proposed in Eq. (23), one may modify formulas of Vaughan and Lye and Dekker as we show below.

1. Vaughan's Formulas

Consider Vaughan's formulas as given by Eqs. (9)-(15). Using Eq. (23), the modified Vaughan's formula would read

$$\delta = \left(ve^{1-v}\right)^k m \ln|pD| e^{\xi(1-\cos\theta)} \quad \text{for} \quad 0 < v \le 3.6$$

$$\delta = \left(\frac{1.125}{v^{0.35}}\right) m \ln|pD| e^{\xi(1-\cos\theta)} \quad \text{for} \quad v > 3.6 . \tag{24}$$

Figure 25 demonstrates the variation of SEY with dose for normal incidence and 45° angle of incidence using the modified Vaughan's formulas (MVF). Note the intersection of the normal incidence and 45° incidence curves for fixed dose.

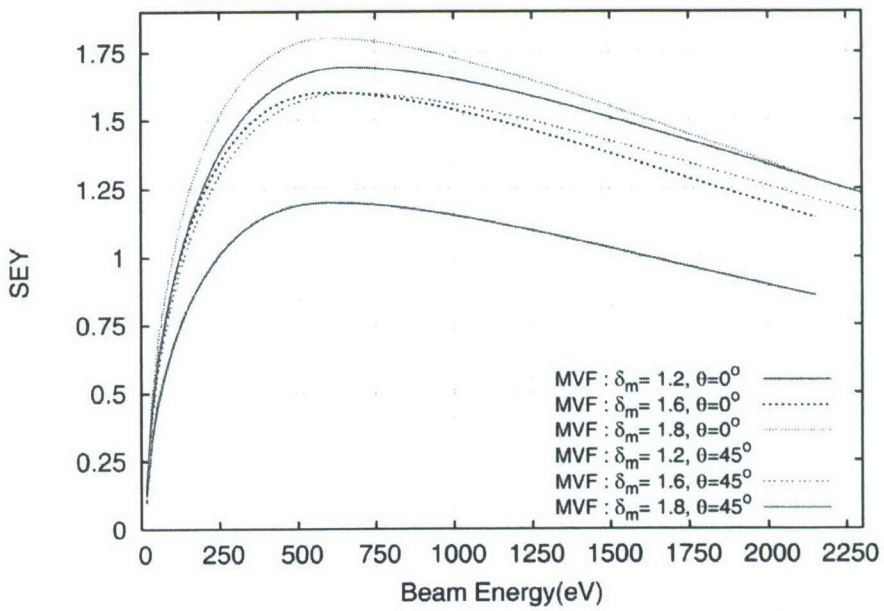

Figure 25. Comparison of SEY as a function of dose for normal incidence and 45° angle of incidence as obtained from the MVF. The incident energy is 600 eV. ξ and m are taken to be 0.5 and 1.0, respectively. δ_m is assumed equivalent to varying the electron dose, as given by Eq. (19).

2. Lee and Dekker's Formulas

Incorporating the dose effect, the modified Lye and Dekker formula would read

$$\delta(\theta) = \frac{1}{g_n(z_m)} g_n\left(z_m \, E_0 / E_{0m}\right) m \ln|pD| e^{\xi(1-\cos\theta)}. \tag{25}$$

In Fig. 26 the SEY curves obtained using the modified Lye-Dekker (MLD) formula for various doses and primary angles of incidence are compared for $n = 0.35$. In contrast to Fig. 25, Fig. 26 indicates SEY curves at different doses do not intersect yield curves at various primary angles of incidence (for the energy range under consideration). The significance of Figs. 25 and 26 will be expounded upon later.

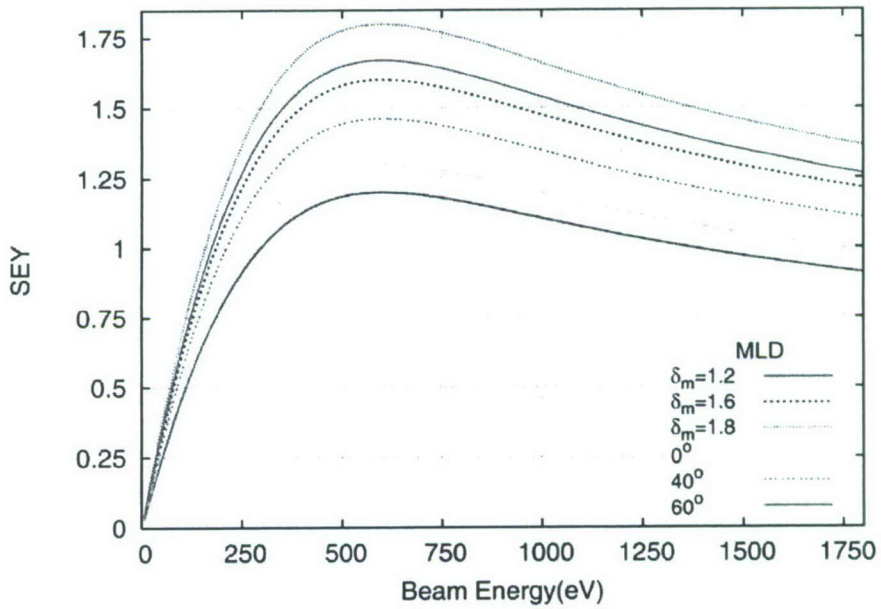

Figure 26. Comparison of SEY as a function of dose for normal incidence, 40° and 60° angles of incidence as obtained from the MLD. The incident energy is 600 eV. ξ and m are taken to be 0.5 and 1.0, respectively. δ_m is assumed equivalent to varying the electron dose, as given by Eq. (19).

3. Discussion

Note, in the formulas above (MVF and MLD), m and p are, in general, functions of energy, angle of incidence, and perhaps other parameters. As an example, suppose one assumes a fit of the form $a + b\ln|D|$ for *all* SEY data points (as opposed to only the maximum SEY considered in Fig. 13. $a + b\ln|D| = m\ln|D| \Rightarrow a = m\ln p$ V and $b = m$. Variation of a and b with primary energy for the data presented in Fig. 11 are shown in Figs. 27 and 28. These figures illustrate a possible nonlinear relationship that may exist between the various coefficients. However, more data is required to accurately determine the functional form and dependencies of these coefficients.

The nature of the relationships functions proposed in Eqs. (24 and 25) are assumed to take

into account the dependence observed in Fig. 12, but, as a consequence, m and p are assumed constant in Figs. 25 and 26.

Previous sections have experimentally established the significance of dose dependence on SEY measurements. It is reasonable to expect an intricate dependence of dose on yield when a theory from first principles is developed. In this regard, modifications to Vaughan's and Lye and Dekker's formulas proposed above must be considered, at best, as a first – if not zeroth order approximation.

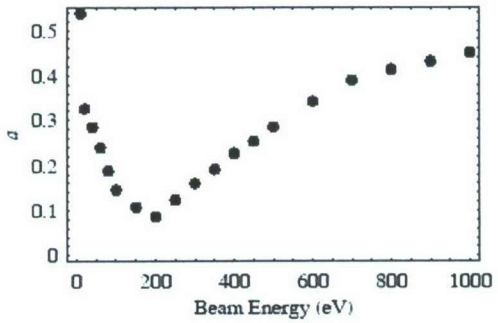

Figure 27. Variation of coefficient a as a function of primary electron energy.

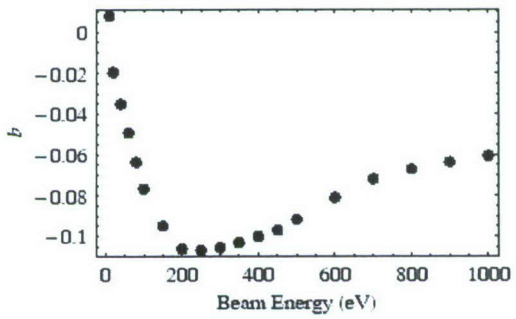

Figure 28. Variation of coefficient b as a function of primary electron energy.

Three important points must be emphasized in regard to the results that have been presented:

- First, the SEY depends on dose at low energies, whereas SEY does not depend on the angle of incidence at low energies, as is observed in experiments.

- Second, it is probable the dose effect influences surface properties (particularly at high doses) which in turn affects SEY. E_{max} in such cases will not remain constant for all doses and will shift depending on surface conditions. This variation/shift is generally unpredictable.

- Third, for any given substance, the SEY remains constant above a given dose D_H and

below a given dose D_L. This defines a "spectrum" of SEY that is unique for that particular substance.

It is beneficial then, to clearly define (experimental) variables on which the SEY of a substance may depend on. As a reminder, such observations are restricted to metals, as with dielectrics, issues such as charging complicate the problem even further.

To begin with, in the most general case, four variables are known to affect SEY in any experiment:

1. Primary electron (beam) energy (E),
2. Angle of incidence of primary electrons (θ),
3. Electron dose (D), and
4. Surface morphology (smoothness) (k_s).

Thus,[6]

$$\delta \equiv \delta(E,\theta,D,k_s). \tag{26}$$

Equation (26) is valid for SEY measurements on pure metals; however, for technical metals a more reasonable dependence would take the form:

$$\delta \equiv \delta(E,\theta,D,k_s,\chi) \tag{27}$$

Where χ denotes the chemical composition of sample surface (pure sample + contaminants). Note, however, for high current density measurements or prolonged exposure to low dose which involve evolution of contaminants due to beam-induced reactions, χ would also appear in Eq. (26).

It remains to be established if the SEY for oblique angles of incidence can be expressed as a smooth function of yield at particular doses. The motivation for exploring such a relationship comes from the following realization: at increasing angles of incidence the area of the electron beam striking the sample surface increases by $\cos(\theta)$, *i.e.,* the net dose decreases and therefore the SEY increases. Therefore, mathematically, it may be possible to consider SEY at a primary angle of incidence as a special case of SEY at a different dose. At first glance MVFs (Fig. 25) seem to indicate that SEY at any angle can be expressed as a *superposition of yields at different doses*. Mathematically, Fig. 25 seems to suggest that a SEY point at (E,θ,D) can be expressed in terms of yield at normal incidence

$$\delta(E,\theta,D) = \sum_{k=0}^{n} \delta(E,0,D_k). \tag{28}$$

[6] Note: δ may additionally depend on constants m and p in Eq. (19).

The MVF also explicitly takes into account low energy angular independence by incorporating quadratic (θ) terms in equations for δ_m and E_m. The MLD formula, on the other hand, suggests SEY at oblique angles of incidence may be a special case of SEY at different doses, *i.e.,* a yield point at (E,θ,D) can be expressed in terms of SEY at normal incidence as

$$\delta(E,\theta,D)=\delta(E,0,D') \tag{29}$$

where $D'\neq D$. The fact that at low energies the SEY yield depends on angle makes the MLD expression questionable. It is likely that a simple $e^{\xi(1-\cos\theta)}$ dependence may not be sufficient to satisfactorily explain SEY at oblique angles of incidence. However, experimental data obtained here seem to agree better with the MLD's formula. Note also that the exponent n in the MLD formula provides large flexibility, as varying n may be considered equivalent to varying surface conditions (the exponent n in Lye and Dekker's formula is related to the range, which will be altered by varying surface morphology). The dose effect is strongly suspected to directly depend on the penetration depth of electrons, but it would be more interesting to observe the variation of scattered secondary electrons as a function of electron dose.

Dionne's formula for δ provides valuable insight by relating SEY to physical microscopic and macroscopic quantities. Incorporating these variables in Eq. (26) provides a more complete description of SEY given by

$$\delta\equiv\delta(E,\theta,D,k_sB,\zeta,\alpha,A,d,n). \tag{30}$$

There is a high probability that one or more of the variables involved are interdependent (for example, the nonlinear relationship between D and E is evident from Fig. 12. Such interdependence would reduce the complexity of the problem significantly. Future research should therefore focus on identifying such relationships.

It is emphasized that SEE is a surface-dependent problem. Results obtained may thus be classified broadly into two categories: 1) SEY of extremely clean samples and 2) SEY of technical materials. The results obtained from technical materials are difficult to reproduce primarily due to difficulty in replicating surface conditions. The first category would serve to enhance fundamental understanding of the physics of SEE while the second category finds more use in practical situations, such as microwave tube collectors, accelerators, *etc.*

With regard to experiments at high current densities, or equivalently, prolonged exposure, the problem is slightly more complicated in that SEY exhibits time-dependent behavior. Notice that Eq. (26) may be written as

$$\delta\equiv\delta(E,\theta,|J|,t,k_s). \tag{31}$$

For experiments at low current densities, time does not play a significant role as opposed to

experiments at high current densities, as demonstrated earlier. For the case of high current densities one may write SEY as

$$\delta \equiv \delta\left(E,\theta,|J_H|,\chi,k_s\right) \tag{32}$$

where J_H denotes high current densities and χ denotes the chemical composition of the surface, which is time-dependent due to beam-induced reactions. Note, J_H implicitly takes into account the variation of SEY due to absolute dose D. Eq. (32) is valid for both pure materials and technical materials.

In computer/numerical simulations of the phenomenon a spectrum of SEY must be considered and evaluated for each particle, for individual primary energy, angle of incidence, dose, and smoothness factor. It would appear that disagreements throughout the hundred-year literature that are often cited as *the* primary cause for the inability to develop a consistent theory are due, at least in part, to the dose effect. Further investigation into this phenomenon would undoubtedly shed light on the physics of SEE.

VII. CONCLUSIONS

An experimental setup has been designed and constructed that allows for the measurement of SEY as a function of beam energy, angle of incidence of primary electrons, electron dose/current density, time, and applied sample bias. The SEY has been measured for copper (Cu), plasma-sprayed boron carbide (PSBC), titanium nitride (TiN), and silver (Ag) samples with principal focus on the dependence on dose.

Based on the results presented here, we observed low current densities to be on the order of 1-500 nA/mm^2 and high current densities to be 1-100 $\mu\,\text{A/mm}^2$. The conclusions summarized below are in specific reference to metals tested in this research and may be applicable to more materials[7]:

1. the total charge/current density incident on a sample's surface significantly affects SEY;
2. the maximum SEY fits well to a relationship of the form $m\ln|D|+c$, where D is the total electron dose and m,c are, in general, functions of primary electron energy and angle of incidence;
3. the prolonged exposure to AGD cleaning may chemically modify the surface of samples, thereby permanently changing δ (this change is dependent on surface chemistry and physics and therefore not predictable);
4. there is a relatively larger variation of SEY with time when using higher current densities. Physio-chemical surface reactions appear to dominate at high current densities (or prolonged exposure to the electron beam), leading to unpredictable behavior in SEY. In such cases it is assumed that the resultant SEY is a convolution of dielectric oxide layers, adventitious carbon, and other (adsorbed) chemicals with the underlying pure metal or even sample substrate;
5. the SEY at low energy does appear to depend on dose, whereas it does not depend on the angle of incidence;
6. the SEY increases with increasing angle of incidence of primary electrons, as predicted by theory. The normalized maximum yields for varying angles of incidence fit better to an exponential dependence of the form $ae^{\xi(1-\cos\theta)}$ (with a,ξ constants) as opposed to a $1/\cos\theta$ dependence.

The results obtained are in good agreement with those published in the literature [2-4]. Discrepancies are believed to be attributed to different electron doses, surface contamination (oxide layers, adsorbed gases, *etc.*), in addition to other factors such as surface morphology and measurement techniques.

[7] All samples are AGD cleaned unless stated otherwise.

VIII. REFERENCES

[1] H. Bruining, *Physics and Applications of Secondary Electron Emission* (Pergamon Press, 1954).

[2] V. Baglin, J. Bojko, O. Gröbner, B. Henrist, N. Hilleret, C. Scheuerlein, M. Taborelli, "The Secondary Electron Yield Of Technical Materials And Its Variation With Surface Treatments," *Proceedings of EPAC 2000* (Vienna, Austria, 2000), pp. 217-221.

[3] R.E. Kirby and F.K. King, SLAC-PUB-8212 (2000).

[4] P.B.M. Lavarec and A. Septier, C. R. Acad. Sci. Paris, vol. T.288 (1979).

[5] N.D. Zameroski, M.S. Thesis, University of New Mexico (Albuquerque, NM, 2004).

[6] J.R.M. Vaughan, IEEE Trans. Electron Dev., vol. 40, p. 830 (1993).

[7] R.G. Lye and A.J. Dekker, Phys. Rev., vol. 107, p. 977 (1957).

[8] E. Baroody, Phys. Rev., vol 78, p. 780 (1950)

[9] G.F. Dionne, J. Appl. Phys., vol. 44, p. 5361 (1973).

[10] G.F. Dionne, J. Appl. Phys., vol. 46, p. 3347 (1975).

[11] J.R.M. Vaughan, IEEE Trans. Electron Dev., vol. 36, p. 1963 (1989).

[12] A. Shih and C. Hor, IEEE Trans. Electron Dev., vol. 40, p. 824 (1993).

[13] R. Kishek and Y.Y. Lau, Phys. Rev. Lett., vol. 80, p. 193 (1998).

[14] V.E. Henrich, Rev. Sci. Instrum., vol. 44, p. 456 (1973).

[15] *ELG-2/EGPS-2 Electron Gun and Power Supply System* (Kimball Physics, Wilton, NH, 2003).

[16] *Model 6514 System Electrometer – Instruction Manual* (Keithley Instruments, Cleveland, OH, 1999).

[17] J.R.M. Vaughan, IEEE Trans. Electron Dev., vol. 35, p. 1172 (1998).

[18] C.M.G.B. Henrist and N. Hilleret, *Proceedings of EPAC 2002* (Paris, France, 2002), pp. 2553-2555.

IX. PERSONNEL, PUBLICATIONS, INTERACTIONS, AWARDS

PERSONNEL

Dr. Edl Schamiloglu	Professor and PI
Dr. Mark Gilmore	Assistant Professor and Co-PI
Mr. Tengiz Svimonishvili	Ph.D. Student
Mr. Prashanth Kumar	M.S. Student
Dr. John Gaudet	Research Professor
Mr. Les Bowers	Research Scholar – providing computational support and interface with AFRL ICEPIC code (2005)

PUBLICATIONS

A. Journal Papers

1. N. D. Zameroski, P. Kumar, C. Watts, T. Svimonishvili, M. Gilmore, E. Schamiloglu, and J. Gaudet, "Experimental Setup and Secondary Electron Yield Measurements from Materials with Application to Collectors of High Power Microwave Devices," IEEE Trans. Plasma Sci. **34**, 642-651 (2006).

2. P. Kumar, C. Watts, T. Svimonishvili, M. Gilmore, and E. Schamiloglu, "The Dose Effect on Secondary Electron Emission," (submitted 2007, in review).

B. Papers in Conference Proceedings

1. E. Schamiloglu, M. Gilmore, C. Watts, J. Gaudet, H. Bosman, T. Svimonishvili, P. Kumar, and N. Zameroski, "Time-Dependent Secondary Electron Yield Measurements from Materials with Application to Depressed Collectors," *Proceedings IVEC 2005* (Noordwijk, The Netherlands, April 2005).

C. Presentations

1. T. Svimonishvili, P. Kumar, L. Bowers, H. Bosman, C. Watts, J. Gaudet, M. Gilmore, and E. Schamiloglu, "Characterization of Materials with Low Secondary Electron Emission Yield for High-Power Microwave Devices," *IEEE International Conference on Plasma Science* (Monterey, CA, June 2005).
2. T. Svimonishvili, C. Watts, E. Schamiloglu, and S. Brueck, "Investigation of the Interaction of an Electron Beam and Metallic Grating in a Smith-Purcell Free Electron Laser (SPFEL)," Bull. Am. Phys. Soc. DPP05, QP1 86 (2005).

3. P. Kumar, T. Svimonishvili, C. Watts, L. Bowers, H. Bosman, M. Gilmore, E. Schamiloglu, and J. Gaudet, "Characterization of Materials (with Low Secondary Electron Emission Yield) for use in High-Power Microwave Devices," Bull. Am. Phys. Soc. DPP05, QP1 104 (2005).
4. P. Kumar, T. Svimonishvili, C. Watts, M. Gilmore, L. Bowers, J. Gaudet, and E. Schamiloglu, "Characterization of Materials with Low Secondary Electron Yield for use in High-power Microwave Devices," *IEEE International Conference on Plasma Science* (Traverse City, MI, June 2006).
5. T. Svimonishvili, E. Schamiloglu, and S. Brueck, "Investigation of the Interaction of an Electron Beam and Metallic Grating in a Smith-Purcell Free Electron Laser (SPFEL)," *IEEE International Conference on Pulsed Power and Plasma Science* (Albuquerque, NM, June 17-22, 2007).
6. P. Kumar, C. Watts, T. Svimonishvili, M. Gilmore, and E. Schamiloglu, "Characterization of the Dose Effect in Secondary Electron Emission," *IEEE International Conference on Pulsed Power and Plasma Science* (Albuquerque, NM, June 17-22, 2007).

INTERACTIONS

Mark Gilmore and Edl Schamiloglu interacted with Dr. Lawrence Ives (Calabazos Creek Research), Dr. Baruch Levush (NRL), Dr. Monica Blank (CPI), and Todd Treado (CPI-Beverly) throughout the course of this project.

Dr. Diana Loree at AFRL authorized SAIC to purchase, on behalf of this UNM effort, a low energy electron gun in order to access the energy range of 5 eV – 1 keV.

The UNM team has been working closely with Dr. Keith Cartwright (AFRL) with the assistance of Mr. Les Bowers in improving the fidelity of the secondary electron emission models in ICEPIC.

RECOGNITION

Professor Mark Gilmore received the 2005 ECE Junior Faculty Researcher of the year award. Professor Edl Schamiloglu was elected an EMP Fellow of the Summa Foundation (2006).

NEW DISCOVERIES, INVENTIONS, PATENTS

None.